Complex Hydrides Li2MH5 (M = B, Al) for Hydrogen Storage Application: Theoretical Study of Structure, Vibrational Spectra and Thermodynamic Properties

Tsere, Melkizedeck Hiiti

Complex Hydrides Li$_2$MH$_5$ (M = B, Al) for Hydrogen Storage Application: Theoretical Study of Structure, Vibrational Spectra and Thermodynamic Properties

Melkizedeck Hiiti Tsere[1, 2, *], Tatiana P. Pogrebnaya[1, 2], Alexander M. Pogrebnoi[1, 2]

[1]The Nelson Mandela African Institution of Science and Technology (NM – AIST), Arusha, Tanzania

[2]Department of Materials, Energy Science and Engineering, the Nelson Mandela African Institution of Science and Technology (NM – AIST), Arusha, Tanzania

Email address:

melkihiiti@yahoo.com (M. H. Tsere), tatiana.pogrebnaya@nm-aist.ac.tz (T. P. Pogrebnaya),
alexander.pogrebnoi@nm-aist.ac.tz (A. M. Pogrebnoi), pgamtp@mail.ru (A. M. Pogrebnoi)

Abstract: Gaseous lithium complex hydrides Li$_2$MH$_5$ (M = B, Al) have been studied using DFT/B3P86 and MP2 methods with 6-311++G(d,p) basis set. High content of hydrogen by these materials accord them with good candidacy as a class of hydrogen storage materials. The optimized geometrical parameters, vibrational spectra and thermodynamic properties of the hydrides and the subunits LiH, Li$_2$H$^+$, Li$_2$H$_2$, MH$_3$, MH$_4^-$, and LiMH$_4$ have been determined. For the LiBH$_4$ the equilibrium configuration was tridentate of C_{3v} symmetry. For LiAlH$_4$ two isomeric forms, bidentate (C_{2v}) and tridentate (C_{3v}), were confirmed to exist, and C_{2v} isomer was shown to dominate in saturated vapor. For complex hydrides Li$_2$MH$_5$, different structural forms were considered but only one asymmetric form (C_1) appeared to be equilibrium. Several possible channels of dissociation of Li$_2$MH$_5$ were considered; the enthalpies and Gibbs free energies of the reactions were computed. The enthalpies of formation $\Delta_fH°(0)$ of the complex hydrides in gaseous phase were determined: -60 ± 10 kJ·mol^{-1} (Li$_2$BH$_5$) and 33 ± 10 kJ·mol^{-1} (Li$_2$AlH$_5$). Heterophase decomposition of the gaseous Li$_2$MH$_5$ with solid products LiH and B/Al and hydrogen gas release was shown to be spontaneous at ambient temperature. Production of hydrogen gas via gaseous decomposition is highly endothermic and achievable at elevated temperatures. The complexes Li$_2$MH$_5$ are therefore proposed to be useful hydrogen storage materials under appropriate conditions.

Keywords: Complex Hydrides, Hydrogen Storage, Geometrical Structure, Vibrational Spectra, Density Functional Theory, Møller–Plesset Perturbation Theory, Basis Set, Isomers, Thermodynamic Properties

1. Introduction

Utilization of hydrogen as fuel energy is limited by lack of viable hydrogen storage materials [1]. Application of hydrogen in fuel cells has an advantage due to the fact that hydrogen is environmentally benign with water as the only byproduct, renewable and has very high energy density compared to any known conventional fuel sources [2, 3]. Also the substantial use of hydrogen as primary fuel energy would greatly reduce the emissions of greenhouse gases and dependence on fossil fuels [4]. Materials suitable for hydrogen storage should have the characteristics such as high capacity to store large weight percent and volumetric fraction of

hydrogen, good desorption/adsorption kinetics as a reversible mechanism [5, 6]. Thermal decomposition of great number of hydrides regarding hydrogen storage application has been discussed in review [7].

Recently, complex hydrides of light weight metals have been reported as prospective materials for hydrogen storage [8]. Thermal stability and reaction reversibility of these hydrides becomes the key barrier for the growth of hydrogen powered fuel cells [9]. However, kinetics of dissociation and formation of these hydrides can be improved by catalytic additives [1]. In 1996, Bogdanovic and Schwickardi [10] first reported on the adsorption and desorption isotherms of catalyzed NaAlH$_4$ at the temperature of around 180°C to 210°C, this has unlocked the researchers' interest towards

lightweight complex metal hydrides as new candidates for hydrogen storage.

Among alkali metals, lithium possesses lowest atomic mass, thus lithium complex hydrides comprise high weight percent of hydrogen. For this reason, $LiBH_4$ and $LiAlH_4$ have been extensively studied as ideal hydrogen storage material [11]. The extreme hydrogen content and decomposition temperature correlated with the electronegativity of metal have been the reason for the growth of the research interest on metal borohydrides [12]. Lithium tetrahydroboride has been discovered by DTA technique in hydrogen at high pressure [13]. Züttel *et al.* [14] proposed decomposition of $LiBH_4$ in liberation of hydrogen gas as

$$LiBH_4 \rightarrow LiH + BH_3 \qquad (1)$$

$$LiBH_4 \rightarrow LiH + B + 3/2H_2 \qquad (2)$$
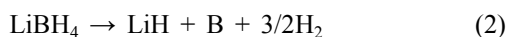
Orimo *et al.* [15] performed the experimental studies and confirmed desorption and rehydrogenation of the compounds mentioned in the Eqs: (1) and (2). The aim of this study is a theoretical investigation of lithium complex hydrides Li_2MH_5 (M = B, Al) in gaseous state. Based on the described decomposition of hydrides in literature [14-16] we suggest the decomposition of Li_2MH_5 to deliver hydrogen in the following reaction steps:

$$Li_2MH_5 \rightarrow LiMH_4 + LiH \qquad (3)$$

$$LiMH_4 \rightarrow LiH + M + 3/2H_2 \qquad (4)$$
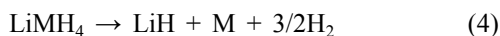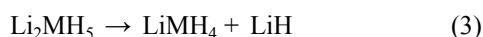
hence Eqs. (3) and (4) can be combined into overall dissociation reaction as shown below:

$$Li_2MH_5 \rightarrow 2LiH + M + 3/2H_2 \qquad (5)$$
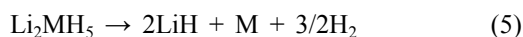
We suggest the decomposition of Li_2MH_5 molecule with elimination of the dimer Li_2H_2 as well:

$$Li_2MH_5 \rightarrow Li_2H_2 + M + 3/2H_2 \qquad (6)$$
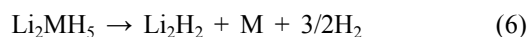
These overall reactions (5) and (6) give the theoretical yield of 10% wt of hydrogen gas when Li_2BH_5 is decomposed and 6.5% wt from decomposition of Li_2AlH_5. The structure, geometrical parameters, vibration spectra and thermodynamic properties of the lithium complex hydrides are to be determined.

2. Methods of Computation and Details of Calculations

Two quantum chemical methods were implemented: namely, density functional theory (DFT) with B3P86 functional and Møller-Plesset perturbation theory of the 2nd order (MP2). The basis set 6-311++G(d,p) was applied in both methods. The General Atomic and Molecular Electronic Structure System (GAMESS) software [17], Firefly version 8.1.0 [18] was used to perform computations. The geometric parameters of the molecules and ions were optimized and the calculations of vibrational frequencies in the harmonic approximation were carried out by the methods implemented in the GAMESS

program. Geometrical structures were analyzed using the ChemCraft software [19]. The thermodynamic functions were determined by using OpenThermo software [20], the thermochemical reference data for calculations were taken from Ivtanthermo Database [21]. The enthalpies of reactions $\Delta_r H°(0)$ were determined through the energies of the reactions $\Delta_r E$ and zero point vibrational energies (ZPVE) $\Delta_r \varepsilon$:

$$\Delta_r H°(0) = \Delta_r E + \Delta_r \varepsilon \qquad (7)$$

$$\Delta_r \varepsilon = 1/2hc(\sum \omega_{i\ prod} - \sum \omega_{i\ react}) \qquad (8)$$

where $\sum \omega_{i\ prod}$ and $\sum \omega_{i\ react}$ are the sum of the vibration frequencies of the products and reactants respectively.

3. Results and Discussion

3.1. Subunits of the Lithium Boron/Aluminium Complex Hydrides

3.1.1. Diatomic Molecules, LiH, H_2, and Triatomic Ion Li_2H^+

The calculated parameters, internuclear distances, ionization energies and the vibrational frequencies, have been calculated and compared with the available reference data so as to analyze the appropriateness of the methods used. The results obtained with both DFT and MP2 methods are in good agreement between each other as well as with the available reference data [22]. As an example, for triatomic ion Li_2H^+ ($D_{\infty h}$) the calculated parameters, equilibrium bond length and vibrational frequencies, are given in Table 1. The MP2 method gives slightly shorter equilibrium internuclear distance and higher frequencies than DFT.

Table 1. *Properties of triatomic ion Li_2H^+ ($D_{\infty h}$).*

Property	DFT/B3P86	MP2	Literature data
R_e (Li-H)	1.649	1.640	1.654 [22]
$-E$	15.44115	15.36474	
$\omega_1(\sum_g^+)$	427 (0)	443 (0)	
$\omega_2(\sum_u^+)$	1663 (12)	1720 (12)	
$\omega_3(\Pi_u)$	391 (22)	404 (24)	

Note: Here and hereafter, R_e are the internuclear distances, Å; E is the total electron energy, au; parenthesized values near frequencies are intensities of IR spectrum bands, D^2 amu^{-1} Å^{-2}, vibrational representation is $\Gamma = \sum_g^+ + \sum_u^+ + \Pi_u$.

3.1.2. Tetraatomic Molecules Li_2H_2, BH_3 and AlH_3

The properties of tetraatomic molecules are presented in Tables 2 and 3, and structures are given in Fig. 1 *a, b*. For the Li_2H_2 molecule, the equilibrium structure is rhomb of D_{2h} symmetry. Molecular parameters are presented in Table 2. Results of computations by DFT and MP2 methods fairly match with each other, and also they are in a very good agreement with quantum chemical data obtained from MP2/6-311++G** and QCISD/6-311++G** methods in [23]. The calculated enthalpies of dimerization are in accordance within uncertainty with the experimental magnitude by Wu and Ihle. [24]. The geometrical structure for BH_3 and AlH_3 is planar of D_{3h} symmetry. For both molecules results obtained by two methods agree well with each other and do not contradict to available literature data [22, 25-30].

Table 2. *Properties of the dimer molecule, Li₂H₂.*

Property	DFT/B3P86	MP2	Literature data
R_e(Li-H)	1.756	1.749	1.758 [23]
α_e(H-Li-H)	99.4	99.5	100 [23]
$-E$	16.22489	16.12348	
$\omega_1 (A_g)$	1158 (0)	1196 (0)	1191 [23]
$\omega_2 (A_g)$	514 (0)	526 (0)	524 [23]
$\omega_3 (B_{1g})$	886 (0)	910 (0)	902 [23]
$\omega_4 (B_{1u})$	591 (18)	607 (19)	604 [23]
$\omega_5 (B_{2u})$	966 (22)	989 (24)	985 [23]
$\omega_6 (B_{3u})$	1063 (22)	1097 (22)	1094 [23]
ΔE_{dim}	−200.9	−207.9	−204 [23]
$\Delta_r H°(0)_{dim}$	−186.7	−193.5	−220 ± 42 [24]

Note: ΔE_{dim} and $\Delta_r H°(0)_{dim}$ are the energy and enthalpy of dimerization reaction 2LiH = Li₂H₂, kJ mol⁻¹; the vibrational representation for Li₂H₂ (D_{2h}) is $\Gamma = 2A_g + B_{1g} + B_{1u} + B_{2u} + B_{3u}$.

3.1.3. Pentaatomic Ions, MH₄⁻

The equilibrium geometrical structure of the ions BH₄⁻ and AlH₄⁻ is tetrahedral of T_d symmetry as shown in Fig. 1 *c*; the properties are represented in Table 4. The calculated properties are also compared with available experimental [31] and theoretical data [32, 33]. The values of R_e(B-H) we obtained do not contradict with the theoretical magnitude 1.239 Å reported by Spoliti *et al.* [32]. Our theoretical internuclear distance R_e(Al-H) is slightly smaller by 0.003 Å (DFT) and 0.014 Å (MP2) than the reference value [33]. The DFT and MP2 results on the frequencies fairly agree with each other with variations of less than 5%. One can note that DFT frequencies better correspond to the experimental values [31].

Table 3. *Properties of the tetraatomic molecules MH₃ (D₃ₕ).*

Properties	BH₃			AlH₃		
	DFT/B3P86	MP2	Reference	DFT/B3P86	MP2	Reference
R_e(M-H)	1.194	1.189	1.190 [25]	1.588	1.575	1.589 [28]
$-E$	26.60572	26.51342		244.18973	243.84355	
$\omega_1 (A_2')$	2533 (0)	2583 (0)	2587 [26]	1937 (0)	2007 (0)	1883 [27]
$\omega_2 (A_2'')$	1143 (2.0)	1182 (2.4)	1148 [28]	708 (8.8)	746 (10.9)	709 [29]
$\omega_3 (E')$	2666 (6.1)	2718 (6.3)	2602 [26]	1949(12.5)	2012 (13.3)	1900 [27]
$\omega_4 (E')$	1185 (0.6)	1243 (0.9)	1197 [26]	791(10.6)	822 (12.7)	783 [30]

Note: The vibrational representation of molecules MH₃ (D_{3h}) is $\Gamma = A_2' + A_2'' + 2E'$.

Table 4. *Properties of pentaatomic anions MH₄⁻ (Td).*

	BH₄⁻			AlH₄⁻		
Properties	DFT/B3P86	MP2	Reference	DFT/B3P86	MP2	Reference
R_e(M-H)	1.241	1.235	1.239 [32]	1.647	1.636	1.650 [32]
$-E$	27.26604	27.14628		244.84829	244.47494	
$\omega_4 (A_1)$	2252 (0)	2312 (0)	2350 [31]	1734 (0)	1805 (0)	1757 [31]
$\omega_2 (E)$	1178 (0)	1218 (0)	1208 [31]	756 (0)	780 (0)	772 [31]
$\omega_3 (T_2)$	2235 (46)	2310 (45)	2250 [31]	1654 (49)	1716 (51.5)	1678 [31]
$\omega_1 (T_2)$	1054 (3.1)	1126 (4.6)	1094 [31]	773 (36)	823 (45)	763 [31]

Notes: In [32], the values R_e for BH₄⁻ and AlH₄⁻ were calculated by MP2/6-31+G*. The vibrational representation for MH₄⁻ (T_d) is $\Gamma = A_1 + E + 2T_2$.
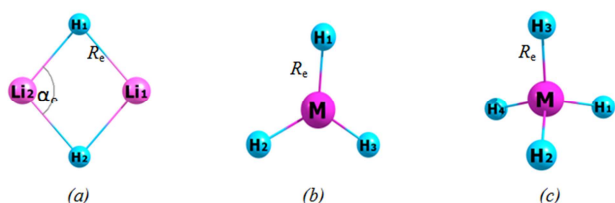
Figure 1. *Equilibrium geometrical structures of the hydride subunits: (a) Li₂H₂ (D₂ₕ); (b) MH₃ (D₃ₕ); (c) MH₄⁻ (Td).*

3.2. Lithium Tetrahydroboride Molecules, LiMH₄

For lithium tetrahydroboride LiMH₄ (M = B, Al), two geometrical configurations were considered; C_{3v} and C_{2v} symmetry (Fig. 2); the geometrical parameters were optimized and the results are given in Tables 5 and 6. By general observations, results obtained by DFT and MP2 are in good correspondence, following the trend inherited from lighter subunits. In a very small deviation, DFT overrates MP2

regarding internuclear distances, but underrates in case of frequencies and dipole moments. The geometrical structure of C_{2v} symmetry for LiBH₄ appeared to be not equilibrium as imaginary frequency $\omega_9 (B_1)$ was observed according to both DFT and MP2 results (Table 6). Therefore the only one equilibrium geometrical structure of C_{3v} symmetry was confirmed for LiBH₄ molecule.

As for LiAlH₄, both structures, of C_{2v} and C_{3v} symmetry, were proved to correspond to minima at the potential energy surface. For the isomerization reaction

$$\text{LiAlH}_4 (C_{3v}) = \text{LiAlH}_4 (C_{2v}) \qquad (9)$$

the values of $\Delta_r E_{iso}$ are negative: −2.4 kJ mol⁻¹ (DFT) and −3.2 kJ mol⁻¹ (MP2), this implies that LiAlH₄ (C_{2v}) isomer is more stable energetically as compared to LiAlH₄ (C_{3v}) isomer. The enthalpy of isomerization reaction calculated using Eqs. (7), (8) are presented in Table 6.

Our results do not contradict with the data calculated by

MP2/6-31G** and MP4/6-31G** methods by Spoliti *et al.* [32], whose findings indicated the imaginary frequencies for the boron complex of C_{2v} symmetry and reported the equilibrium structure of C_{3v} symmetry for LiBH$_4$. The existence of two stable configurations of C_{2v} and C_{3v} for LiAlH$_4$ molecule was found in [32] and shown that the C_{2v} isomer was more stable energetically than C_{3v}, the energy of separation between the two isomers was small, 1.6 kJ mol^{-1}.

The IR spectra of LiMH$_4$ molecules are presented in Figs. 3 and 4. Close observation of these spectra reveals common characteristic vibrational modes for the same isomers (C_{3v}) of LiBH$_4$ and LiAlH$_4$ (Figs. 3 *a*, *b*). For example, the most intensive bands at 2220 cm^{-1} for LiBH$_4$ and 1606 cm^{-1} for LiAlH$_4$ are assigned to asymmetrical stretching H$_3$-B-H$_4$ and

H$_3$-Al-H$_4$, respectively. On the other hand in spectrum of LiAlH$_4$ modes of high intensity appear at the 954 cm^{-1} (Li-H$_2$, Li-H$_3$ and Li-H$_4$) and the 779 cm^{-1} (H$_1$-Al) in contrast to spectrum of LiBH$_4$ where similar bands are not seen due to low intensities.

As for the IR spectrum of the C_{2v} LiAlH$_4$ isomer (Fig. 4), it looks quite different compared to that of C_{3v} isomer. The former has many intensive bands, including symmetrical stretching at the 1897 cm^{-1} (H$_1$-Al-H$_2$), 1161 cm^{-1} (H$_3$-Li-H$_4$), asymmetrical stretching at the 1032 cm^{-1} (H$_3$-Li-H$_4$), scissoring at the 1556 cm^{-1} (H$_3$-Li-H$_4$), rocking at the 1441 cm^{-1} (H$_3$-Li-H$_4$) and wagging mode at the 810 cm^{-1} (H$_3$-Li-H$_4$).

(a)   *(b)*

Figure 2. *Equilibrium geometrical structures of hexaatomic isomers LiMH$_4$: (a) LiMH$_4$ (C_{3v}); (b) LiAlH$_4$ (C_{2v}).*

Table 5. *Properties of hexaatomic molecules, LiMH$_4$ (C_{3v}).*

	LiBH$_4$		LiAlH$_4$	
Properties	DFT/B3P86	MP2	DFT/B3P86	MP2
R_{e1}(H$_1$-M)	1.196	1.192	1.581	1.569
R_{e2}(H$_2$-M)	1.248	1.243	1.665	1.654
R_{e3}(H$_2$-Li)	1.837	1.831	1.933	1.920
α_1	105.7	105.5	93.3	93.1
α_2	74.3	74.7	76.6	76.8
α_3	65.6	65.4	77.5	77.4
$-E$	34.78829	34.64343	252.34624	251.94888
ω_1 (A_1)	2588 (2.9)	2653 (3.2)	1958 (3.6)	2032 (4.0)
ω_2 (A_1)	2242 (3.4)	2297 (3.6)	1710 (5.7)	1786 (6.2)
ω_3 (A_1)	1215 (2.3)	1282 (2.9)	954 (13.6)	1007 (15.5)
ω_4 (A_1)	693 (3.9)	706 (4.0)	547 (2.6)	563 (2.6)
ω_5 (E)	2220 (16.0)	2280 (16.1)	1606 (18.5)	1670 (19.7)
ω_6 (E)	1266 (0.1)	1324 (0.2)	876 (4.6)	932 (7.3)
ω_7 (E)	1097 (1.3)	1159 (1.7)	779 (12.9)	820 (14.3)
ω_8 (E)	496 (0.1)	519 (0.1)	334 (0.05)	352 (0.09)
μ_e	6.0	6.2	4.6	4.6

Note: μ_e is the dipole moment in D; vibrational representation for molecules LiMH$_4$ (C_{3v}) is $\Gamma = 4A_1 + 4E$.

Table 6. *Properties of hexaatomic molecules LiMH$_4$ (C_{2v}).*

	LiBH$_4$		LiAlH$_4$	
Properties	DFT/B3P86	MP2	DFT/B3P86	MP2
R_{e1}(H$_1$-M)	1.209	1.204	1.597	1.585
R_{e2}(H$_2$-M)	1.262	1.256	1.703	1.690
R_{e3}(H$_2$-Li)	1.705	1.703	1.756	1.748
α_1	109.4	108.7	90.5	90.1
α_2	88.1	88.8	91.2	91.8
α_3	74.3	73.7	87.1	86.4
α_4	114.6	114.8	121.6	121.4
$-E$	34.77992	34.63433	252.34739	251.95012

	LiBH$_4$		LiAlH$_4$	
Properties	DFT/B3P86	MP2	DFT/B3P86	MP2
$\Delta_r E_{iso}$			−3.0	−3.2
$\Delta_r H°(0)_{iso}$			−2.4	−3.1
ω_1 (A_1)	2465 (2.1)	2524 (2.4)	1897 (1.9)	1966 (2.1)
ω_2 (A_1)	2121 (7.7)	2182 (8.2)	1556 (11.0)	1622 (12.2)
ω_3 (A_1)	1410 (2.9)	1471 (3.1)	1161 (10.2)	1211 (11.4)
ω_4 (A_1)	609 (2.7)	617 (2.8)	742 (5.1)	780 (6.3)
ω_5 (A_1)	1118 (0.6)	1180 (0.8)	477 (1.3)	491 (1.3)
ω_6 (A_2)	1166 (0)	1207 (0)	700 (0)	720 (0)
ω_7 (B_1)	2510 (4.2)	2575 (4.5)	1894 (7.4)	1961 (8.2)
ω_8 (B_1)	1032 (0.2)	1099 (0.4)	810 (8.3)	853 (10.3)
ω_9 (B_1)	230 (i) (0.6)	234 (i) (0.6)	187 (0.2)	198 (0.2)
ω_{10} (B_2)	2112 (10.9)	2175 (11.2)	1441 (11.0)	1493 (11.4)
ω_{11} (B_2)	1260 (1.0)	1308 (1.3)	1032 (6.6)	1068 (8.7)
ω_{12} (B_2)	761 (0.001)	784 (0.001)	562 (2.9)	586 (3.4)
μ_e	6.9	7.2	6.3	6.5

Note: $\Delta_r E_{iso}$ and $\Delta_r H°(0)_{iso}$ are the energy and enthalpy of isomerization reaction LiAlH$_4$ (C$_{3v}$) = LiAlH$_4$ (C$_{2v}$), in kJ·mol^{-1}. Vibrational representation for molecules LiMH$_4$ (C$_{2v}$) is $\Gamma = 5A_1 + A_2 + 3B_1 + 3B_2$.
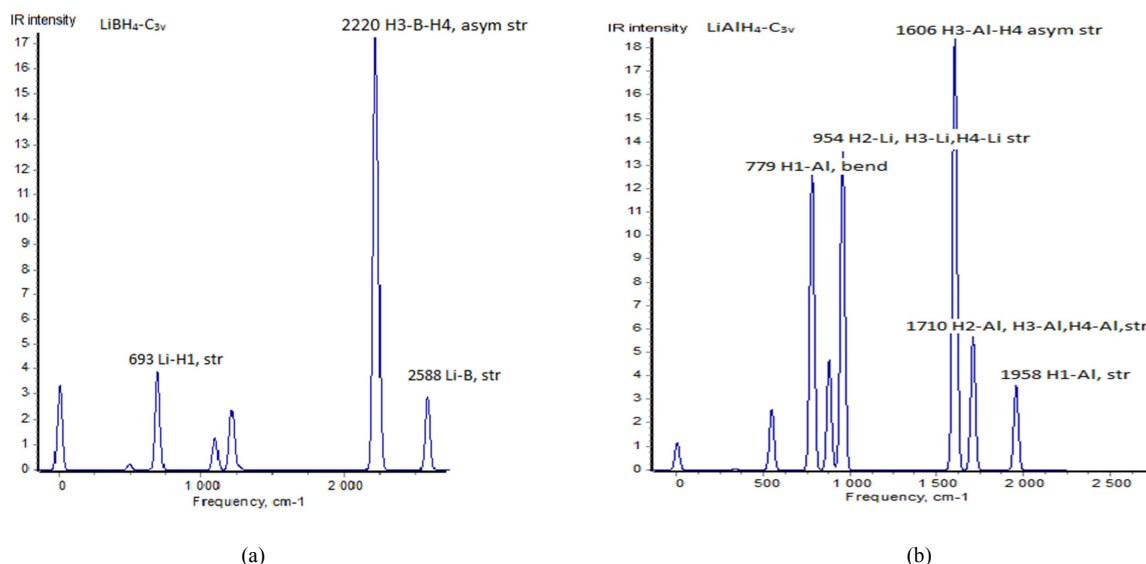

Figure 3. *Infrared spectra of hexaatomic molecules LiMH$_4$ (DFT/B3P86): (a) LiBH$_4$ (C$_{3v}$); (b) LiAlH$_4$ (C$_{3v}$).*
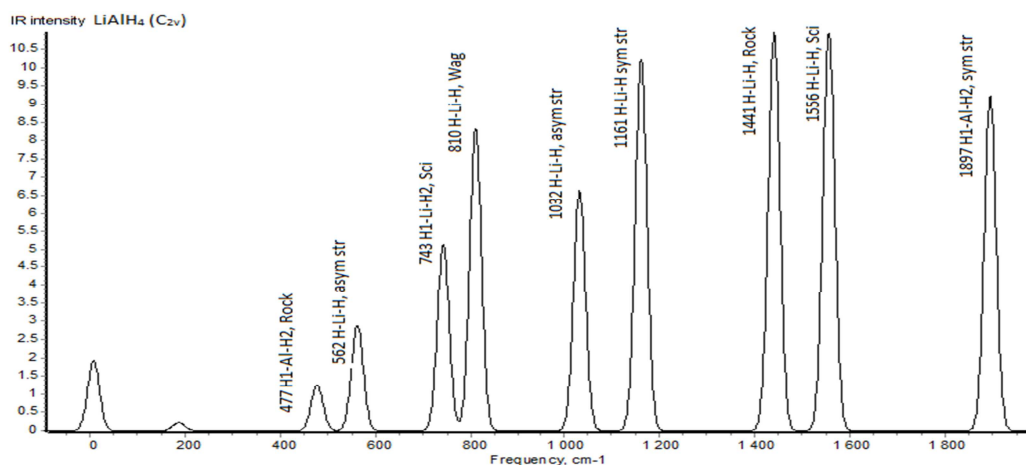

Figure 4. *Infrared spectrum of LiAlH$_4$ (C$_{2v}$) isomer (DFT/B3P86).*

To evaluate the relative content of the isomers of the LiAlH$_4$ molecule, the thermodynamic approach was applied. The pressure ratio $p(C_{2v})/p(C_{3v})$ of two isomers in the equilibrium vapour was determined using the equation

$$\Delta_r H°(0) = -RT\ln[p(C_{2v})/p(C_{3v})] + T\Delta_r\Phi°(T) \qquad (10)$$

where $\Delta_r H°(0)$ is the enthalpy of the isomerization reaction (9); T is absolute temperature; $\Delta_r\Phi°(T)$ is the reduced Gibbs energy of the reaction, $\Phi°(T) = -[H°(T)-H°(0)-TS°(T)]/T$. The values of $\Phi°(T)$ and other thermodynamic functions were calculated using the optimized geometrical parameters and vibrational frequencies obtained by both DFT/B3P86 and MP2 method. The temperature effect on the concentrations of these isomers were also considered and plotted in Fig. 5. As is seen the isomer C_{2v} is more abundant than that of C_{3v} symmetry. For example, at 1000 K the $p(C_{2v})/p(C_{3v})$ is about 3−3.5. As the temperature raises the ratio decreases, still the C_{2v} isomer remains the prevailing for whole temperature range considered.
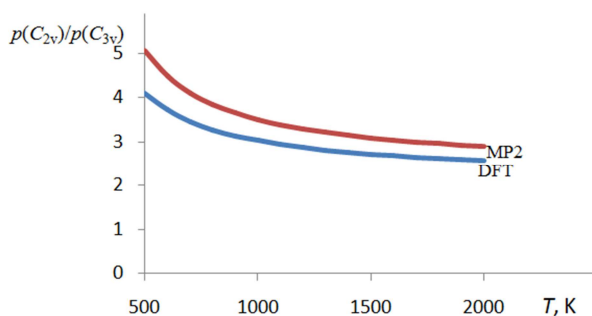

Figure 5. *Relative abundance of two isomers of LiAlH4, p(C2v)/p(C3v).*

3.3. Geometrical Structure and Vibrational Spectra of Complex Hydride Molecules, Li₂MH₅

Two possible geometrical configurations of C_{2v} and C_1 symmetry were considered for octaatomic Li_2BH_5 and Li_2AlH_5 molecules. For the C_{2v} structure, the imaginary frequencies were revealed through calculations using both methods DFT and MP2, and this structure was not taken for further consideration. Thus only one equilibrium configuration of the Li_2MH_5 molecules was proved to exist, namely the asymmetrical structure of the C_1 point group (Fig. 6).
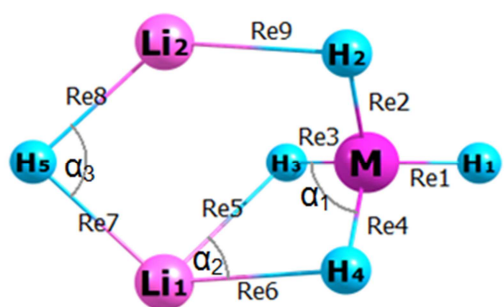

Figure 6. *Equilibrium geometrical structure of octaaomic molecules Li2MH5 (C1).*

The geometrical parameters are given in Table 7. The results revealed a good agreement between two methods. The internuclear distances by DFT method overrate those by MP2; the difference is in the range 0.003–0.012 Å. These deviations are within the range depicted above for lower species whose parameters have been compared with reference data. The frequencies obtained by MP2 overrate those by DFT in

accordance to the general trend as it was shown above for the lighter species. The IR spectra for the octaatomic complex hydrides Li_2MH_5 (M = B, Al) are shown in Fig. 7. In the spectrum of Li_2BH_5, the stretching modes of high intensities are observed at 1008 cm⁻¹ and 2287 cm⁻¹ and bending mode H3-Li-H5 at 452 cm⁻¹.

Table 7. *Properties of octaatomic molecules Li₂MH₅ (C₁).*

Properties	Li₂BH₅		Li₂AlH₅	
	DFT/ B3P86	MP2	DFT/ B3P86	MP2
R_{e1}	1.202	1.197	1.588	1.576
R_{e2}	1.238	1.233	1.663	1.652
R_{e3}	1.247	1.242	1.654	1.644
R_{e4}	1.238	1.233	1.654	1.642
R_{e5}	1.961	1.960	1.939	1.936
R_{e6}	1.819	1.813	1.941	1.922
R_{e7}	1.723	1.715	1.721	1.716
R_{e8}	1.723	1.715	1.690	1.685
R_{e9}	1.821	1.813	1.784	1.772
α_1	109.3	108.8	95.9	95.4
α_2	64.7	64.3	78.5	78.1
α_3	89.2	89.6	102.5	102.8
$-E$	42.93156	42.73818	260.49404	260.04852
ω_1	99	129	99	59
ω_2	333	336	253	264
ω_3	426	433	316	326
ω_4	452	458	366	379
ω_5	486	500	410	422
ω_6	528	546	461	475
ω_7	560	576	463	482
ω_8	1066	1105	773	810
ω_9	1074	1133	775	819
ω_{10}	1108	1148	832	872
ω_{11}	1120	1177	961	1004
ω_{12}	1211	1268	1002	1032
ω_{13}	1255	1315	1036	1083
ω_{14}	1338	1395	1221	1255
ω_{15}	2236	2290	1631	1697
ω_{16}	2277	2337	1641	1710
ω_{17}	2287	2351	1718	1795
ω_{18}	2544	2609	1933	2002
μ_e	2.8	2.0	2.7	2.6

In spectrum of Li_2AlH_5 molecule, high intensity peaks correspond to the stretching and wagging vibrational modes. The most intensive asymmetrical stretching modes appear at 1641 cm⁻¹ (H2-Al-H3), 832 cm⁻¹ (H3-Li1-H4) and 1222 cm⁻¹ (Li1-H5-Li2); symmetrical vibrations are observed at 1002 cm⁻¹ (Li1-H5-Li2) and 1718 cm⁻¹ (H3-Al-H4). Wagging vibrational modes appear at 461 cm⁻¹ (Li-H5-Li2) and 773 cm⁻¹ (H3-Al-H4). Worth to note the spectra of two molecules Li_2BH_5 and Li_2AlH_5 are not completely imposable and this signifies that the spectra exhibit specific features regardless the similarity of geometrical shape of the molecules.

3.4. The Enthalpies of Dissociation Reactions and Enthalpies of Formation of Complex Hydride Molecules Li₂MH₅

Several possible dissociation reactions of complex hydrides were considered. Theoretical enthalpies of reactions were determined according to Eqs. (7), (8). The reaction equations, energies, ZPVE corrections, enthalpies of the gaseous

reactions and enthalpies of formation of the complex hydride molecules are presented in Table 8. A partial dissociation of Li$_2$MH$_5$ without release of hydrogen gas is described by reactions (i)-(iv) for Li$_2$BH$_5$ and (vi)-(ix) for Li$_2$AlH$_5$; while reactions (v) and (x) correspond to the complete reduction of boron or aluminium accompanied by hydrogen gas evolving. As is seen all dissociation reactions proceed with absorption of heat (endothermic reactions). For partial dissociation reactions leading to the formation of hydrides, LiH and LiMH$_4$, lower energy is required than for other reactions.

Enthalpies of formation of complex hydrides in gaseous state were determined using the formula

$$\Delta_r H^\circ(0) = \sum \Delta_f H^\circ(0)_{prod} - \sum \Delta_f H^\circ(0)_{react} \qquad (11)$$

where $\Delta_r H^\circ(0)$ is the enthalpy of reaction, $\Delta_f H^\circ(0)_{prod}$ and $\Delta_f H^\circ(0)_{react}$ are enthalpies of formation of products and reactants, respectively. The values of $\Delta_f H^\circ(0)_{prod}$ for gaseous LiH, BH$_3$, AlH$_3$, B, and Al were taken from Ivtanthermo Database [17]. The enthalpy of formation of the gaseous Li$_2$H$_2$ molecule, $\Delta_f H^\circ(0) = 85.4$ kJ mol^{-1} was estimated through the enthalpy of dimerization (-193.5 kJ mol^{-1}, MP2, shown above

in Table 2). The enthalpies of formation of the complex hydride molecules were calculated by both DFT and MP2 methods. For the hexaatomic molecules LiMH$_4$, the enthalpies of formation were calculated through reactions (i) and (vi); the averaged values obtained by DFT and MP2 methods were: -27 ± 6 kJ mol^{-1} (LiBH$_4$) and 74 ± 6 kJ mol^{-1} (LiAlH$_4$). For each complex hydride molecule Li$_2$MH$_5$, three reactions were taken into account: (ii), (iii), (v) for Li$_2$BH$_5$ and (vii), (viii), (x) for Li$_2$AlH$_5$. The accepted averaged values of $\Delta_f H^\circ(0)$ were: -60 ± 10 kJ mol^{-1} (Li$_2$BH$_5$) and 33 ± 10 kJ mol^{-1} (Li$_2$AlH$_5$). Uncertainties were estimated as half-difference between maximum and minimum magnitudes.

The heterophase reactions were also considered. Using the reference datum of $\Delta_f H^\circ$(LiH, c, 0 K) [17] and enthalpies of formation of the gaseous Li$_2$MH$_5$, the enthalpies of heterophase reactions were calculated (Table 9). Two types of the reactions may be seen. In the first one, where boron or aluminium is in solid state and LiH is in the gaseous phase, the enthalpies are positive. In the reactions of the second type where two products, LiH and B or Al, are in condensed phase, enthalpies are negative, *i.e.* these reactions are exothermic.

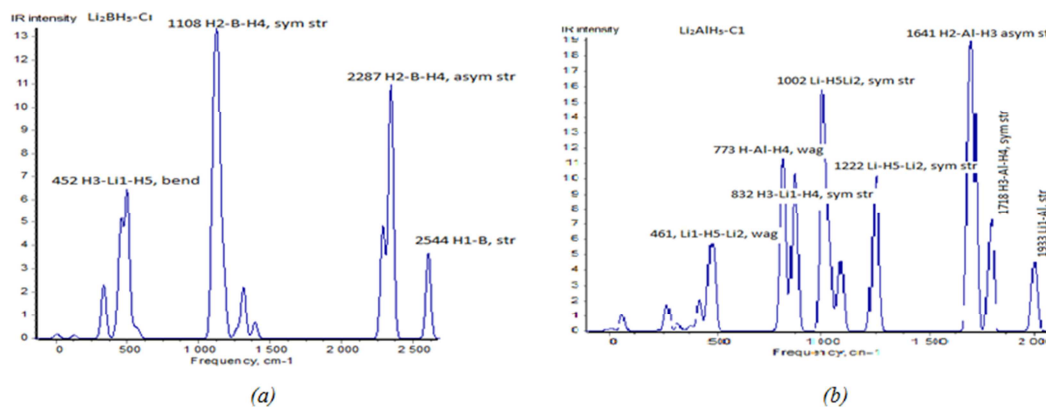**Figure 7.** *Infrared spectra of octaatomic molecules Li$_2$MH$_5$ (C$_1$) calculated by DFT/B3P86: (a) Li$_2$BH$_5$; (b) Li$_2$AlH$_5$.*

Table 8. *The gas phase dissociation reactions, energies $\Delta_r E$, ZPVE corrections $\Delta_r \varepsilon$, enthalpies of the reactions $\Delta_r H^\circ(0)$ and enthalpies of formation $\Delta_f H^\circ(0)$ of the complex hydride molecules (in kJ mol^{-1}).*

	Gas Phase Reaction	Method	$\Delta_r E$	$\Delta_r \varepsilon$	$\Delta_r H^\circ(0)$	$\Delta_f H^\circ(0)$
i	LiBH$_4$ = LiH + BH$_3$	DFT	284.6	−24.7	259.9	−28.6
		MP2	283.2	−26.2	257.0	−25.6
ii	Li$_2$BH$_5$ = LiH + LiBH$_4$	DFT	181.4	−12.6	168.8	−57.9
		MP2	190.6	−13.0	177.7	−51.1
iii	Li$_2$BH$_5$ = Li$_2$H$_2$ + BH$_3$	DFT	265.0	−23.0	242.0	−67.2
		MP2	265.9	−24.5	241.4	−66.6
iv	Li$_2$BH$_5$ = Li$_2$H$^+$ + BH$_4^-$	DFT	589.1	−20.6	568.5	
		MP2	596.4	−20.9	575.6	
v	Li$_2$BH$_5$ = 2LiH + B + 3/2H$_2$	DFT	970.5	−65.9	904.6	−65.8
		MP2	960.6	−68.4	892.2	−53.4
vi	LiAlH$_4$ = LiH+ AlH$_3$	DFT	216.1	−16.9	199.2	76.0
		MP2	221.6	−18.5	203.1	72.0
vii	Li$_2$AlH$_5$ = LiH+ LiAlH$_4$	DFT	190.3	−12.2	178.1	37.3
		MP2	200.2	−12.6	187.7	23.8
viii	Li$_2$AlH$_5$ = Li$_2$H$_2$ + AlH$_3$	DFT	208.5	−15.5	193.0	25.6
		MP2	213.9	−16.4	197.6	21.0
ix	Li$_2$AlH$_5$ = Li$_2$H$^+$ + AlH$_4^-$	DFT	537.2	−14.9	522.2	
		MP2	548.3	−15.2	533.2	
x	Li$_2$AlH$_5$ = 2LiH + Al + 3/2H$_2$	DFT	607.6	−38.9	568.6	37.9
		MP2	614.7	−40.8	573.9	32.6

Table 9. *Enthalpies of heterophase reactions (in kJ mol^{-1}).*

Heterophase reaction	$\Delta_r H°(0)$
$Li_2BH_{5\ (g)} = 2LiH_{(g)} + B_{(s)} + 3/2H_{2\ (g)}$	339
$Li_2BH_{5\ (g)} = 2LiH_{(s)} + B_{(s)} + 3/2H_{2\ (g)}$	−111
$Li_2AlH_{5\ (g)} = 2LiH_{(g)} + Al_{(s)} + 3/2H_{2\ (g)}$	246
$Li_2AlH_{5\ (g)} = 2LiH_{(s)} + Al_{(s)} + 3/2H_{2\ (g)}$	−204

3.5. Thermal Stability of the Complex Hydrides, Li_2MH_5

The thermal stability of the complex hydrides was examined on the base of the Gibbs free energies for the dissociation reactions; the values of $\Delta_r G°(T)$ were considered as a quantitative measure of the chemical processes favorability. The Gibbs free energies were calculated by using the expression:

$$\Delta_r G°(T) = \Delta_r H°(T) - T\Delta_r S°(T) \qquad (12)$$

The required thermodynamic functions have been computed using a rigid rotator-harmonic oscillator approximation, based on geometrical parameters and vibrational frequencies calculated by DFT/B3P86 method. Among several proposed partial dissociation channels (Table 8), two types of gas phase reactions were chosen for examination of Gibbs free energy temperature dependence. Reactions (ii) and (vii) in which the complexes Li_2MH_5 decompose into LiH and $LiMH_4$, were chosen (Fig. 8 *a*) as they expected to be favorable due to lower enthalpies of the reactions. Another type of the processes relates to the reactions (v) and (x), in which Li_2MH_5 complex hydrides decompose into gaseous products LiH, M, and H_2; the plots of $\Delta_r G°(T)$ are shown in Fig. 8 *b*.

As is seen, the decomposition of Li_2BH_5 into LiH and LiBH$_4$ is thermodynamically favored at temperature above 1300 K, while for Li_2AlH_5 the spontaneous partial dissociation into LiH and $LiAlH_4$ occurs at 1700 K and above. This implies that, the formation of intermediate product $LiBH_4$ is rather preferred compared to $LiAlH_4$; this result is in accordance with lower value of enthalpy of dissociation of Li_2BH_5 compared to Li_2AlH_5. For gas phase channels with hydrogen evulsion, reactions become spontaneous at relatively elevated temperature, *i.e.* at about 2250 K for Li_2BH_5 and 1500 K for Li_2AlH_5, respectively (Fig. 8 *b*). Below these temperatures the systems favor the reverse reactions which lead to the formation of reactants Li_2MH_5.

It is worth to compare the two gas phase dissociation channels for the same complex hydride. For Li_2BH_5 the spontaneous decomposition into LiH and $LiBH_4$ starts at 1300 while in the second type of decomposition, hydrogen gas is not evolved at temperature below ~2200 K. For Li_2AlH_5, the formation of intermediate products (LiH and $LiAlH_4$) occurs at 1700 K which is relatively higher as compared to complete dissociation which becomes spontaneous at 1500 K. Therefore the results show both complexes, Li_2BH_5 and Li_2AlH_5, are stable for the partial decomposition and hydrogen evolving reactions in a broad temperature range.

Gibbs free energy $\Delta_r G°(T)$ for heterophase reactions were also considered and shown in Figs. 9 *a, b*. First part of the graph (Fig. 9 *a*) represents the reactions where only one product (B or Al) is maintained in condensed state. The dissociation reactions become spontaneous at elevated temperatures ~1300 K (Li_2BH_5) and ~1000 K (Li_2AlH_5); below these temperatures the values of $\Delta_r G°(T)$ are positive, thus reverse reactions are predicted to be spontaneous. For the reactions in which the products except hydrogen are kept in a solid form, the values of $\Delta_r G°(T)$ are negative for whole temperature range considered (Fig. 9 *b*).

(a)

(b)
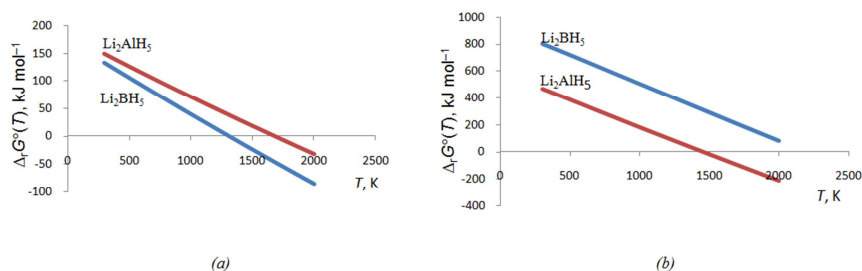
Figure 8. *Gibbs energy vs. temperature for gas-phase decomposition of complex hydrides Li_2MH_5: (a) partial dissociation $Li_2MH_5 = 2LiH + LiMH_4$; (b) $Li_2MH_5 = 2LiH + M + 3/2H_2$.*

(a)

(b)
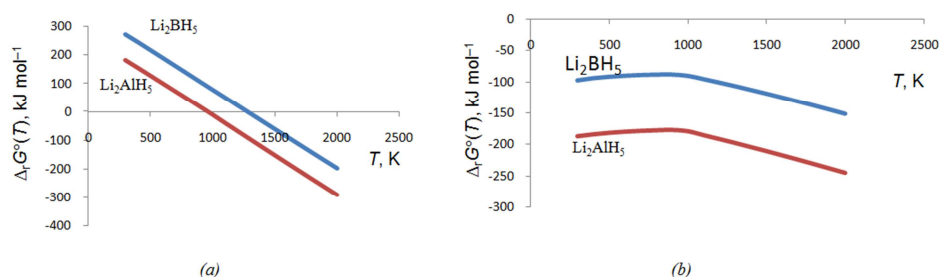
Figure 9. *Gibbs energy vs. temperature for heterophase decomposition of complex hydrides Li_2MH_5: (a) $Li_2MH_{5(g)} = 2LiH_{(g)} + M_{(s)} + 3/2H_2$; (b) $Li_2MH_{5(g)} = 2LiH_{(s)} + M_{(s)} + 3/2H_{2(g)}$.*

These graphs indicate that complex hydrides Li$_2$MH$_5$ can dissociate even at room temperature to produce hydrogen gas. For Li$_2$AlH$_5$ complex Gibbs energies are more negative than for Li$_2$BH$_5$, that relates to bigger exothermicity of dissociation reaction for the former: $\Delta_r H°(0)$ equals to –204 kJ mol^{-1} (Li$_2$AlH$_5$) and –111 kJ mol^{-1} (Li$_2$BH$_5$). The inflection on both curves corresponds to the melting point of lithium hydride that is 965 K [17]. If compare two heterogeneous channels it is evident that the reactions in which all products except hydrogen are solid, are more favorable for hydrogen gas evolving due to the spontaneity of the process.

Compared to gas phase dissociation, heterophase reactions are more appropriate for the purpose of producing hydrogen gas. The complex hydrides decompose spontaneously into solid products and hydrogen gas at standard conditions. On the other hand the thermal instability of the Li$_2$MH$_5$ species turns into a disadvantage of these materials because the reverse reaction seems difficult to be carried out. The stabilization of the complex hydrides Li$_2$MH$_5$ may be achieved by applying special technique e.g. matrix isolation [4] or increasing the pressure in the system.

4. Conclusion

The geometrical parameters, vibrational frequencies and thermodynamic properties of the complex gaseous hydrides Li$_2$BH$_5$ and Li$_2$AlH$_5$ have been theoretically determined using DFT/B3P86 and MP2 methods. The same methods were applied to compute the properties of the lower species considered as subunits of the complexes. The results obtained by DFT and MP2 methods are in good correspondence between each other; also good accordance was observed in the reference data available for lower species. The different possible channels of Li$_2$MH$_5$ decomposition have been examined. The enthalpies and Gibbs energies of dissociation reactions were calculated and analyzed. High stability of these complex hydrides regarding the decomposition into gaseous products was shown. However, spontaneous dissociation was revealed for the heterophase decomposition into solid products LiH and B/Al and hydrogen gas evolving. From our speculations based on a thermodynamic approach we can suggest the complexes Li$_2$BH$_5$ and Li$_2$AlH$_5$ may be potential materials for hydrogen storage application, provided the stabilization of them and reversibility of dehydrogenization process are achievable.

Acknowledgment

Authors' Contributions

Authors participated equally in all steps to the completion of this work.

References

[1] Delmelle, R., Gehrig, J. C., Borgschulte, A. & Züttel, A. Reactivity enhancement of oxide skins in reversible Ti-doped NaAlH$_4$. AIP Adv. 4, 127130 (2014).

[2] Yang, J., Sudik, A., Wolverton, C. & Siegel, D. J. High capacity hydrogen storage materials: attributes for automotive applications and techniques for materials discovery. Chem. Soc. Rev. 39, 656–675 (2010).

[3] Pottmaier, D. & Baricco, M. Materials for hydrogen storage and the Na-Mg-B-H system. AIMS Energy 3, 75–100 (2015).

[4] Zhang, T., Isobe, S., Wang, Y., Oka, H., Hashimoto, N. & Ohnuki, S. A metal-oxide catalyst enhanced the desorption properties in complex metal hydrides. J. Mater. Chem. A 2, 4361 (2014).

[5] Sundqvist, B. Pressure-temperature phase relations in complex hydrides. in Solid State Phenomena 150, 175–195 (Trans Tech Publ, 2009).

[6] Seayad, A. M. & Antonelli, D. M. Recent Advances in Hydrogen Storage in Metal-Containing Inorganic Nanostructures and Related Materials. Adv. Mater. 16, 765–777 (2004).

[7] Grochala, W. & Edwards, P. P. Thermal Decomposition of the Non-Intersitial Hydrides for the Storage and Production of Hydrogen. Chem. Rev. 104, p1283 – 1315 (2004).

[8] Dovgaliuk, I., Le Duff, C. S., Robeyns, K., Devillers, M. & Filinchuk, Y. Mild Dehydrogenation of Ammonia Borane Complexed with Aluminum Borohydride. Chem. Mater. 27, 768–777 (2015).

[9] Jaroń, T., Wegner, W. & Grochala, W. M[Y(BH$_4$)$_4$] and M$_2$Li [Y(BH$_4$)$_{6-x}$Cl$_x$] (M = Rb, Cs): new borohydride derivatives of yttrium and their hydrogen storage properties. Dalt. Trans., 42, 6886-6893. (2013).

[10] Bogdanović, B. & Schwickardi, M. Ti-doped alkali metal aluminium hydrides as potential novel reversible hydrogen storage materials. J. Alloys Compd. 253, 1–9 (1997).

[11] Goudon, J. P., Bernard, F., Renouard, J. & Yvart, P. Experimental investigation on lithium borohydride hydrolysis. Int. J. Hydrogen Energy 35, 11071–11076 (2010).

[12] Ley M. B., Jepsen, L. H., Lee, Y. S., Cho, Y. W., Bellosta von Colbe, J. M., Dornheim, M., Rokni, M., Jensen, J. O.,Sloth M., Filinchuk, Y., Jørgensen, J. E., Besenbacher, F. & Jensen, T. R. Complex hydrides for hydrogen storage–new perspectives. Mater. Today 17, 122-128 (2014).

[13] Stasinevich, D. & Egorenko, G. Thermographic investigation of alkali metal and magnesium tetrahydroborates at pressures up to 10 atm. Russ. J. Inorg. Chem., 13, 341-343 (1968).

[14] Züttel, A., Wenger, P., Rentsch, S., Sudan, P., Mauron, Ph., and Emmenegger, Ch. Hydrogen storage properties of LiBH$_4$. J. Alloys Compd. 356, 515–520 (2003).

[15] Orimo, S., Nakamori, Y. & Kitahara, G. Dehydriding and rehydriding reactions of LiBH$_4$. J. Alloys Compd. 404-406, 427-430 (2005).

[16] Gross, K. J., Thomas, G. J. & Jensen, C. M. Catalyzed alanates for hydrogen storage. J. Alloys Compd. 330-332, 683–690 (2002).

[17] Schmidt M. W., Baldridge K. K., Boatz J. A., Elbert S. T., Gordon M. S., Jensen J. H., Koseki S., Matsunaga N., Nguyen K. A., Su S., Windus T. L., Dupuis M., Montgomery J. A. "General Atomic and Molecular Electronic Structure System". J. Comput. Chem. 1993; 14:1347-1363; doi: 10.1002/jcc. 540141112.

[18] Granovsky, A. A. Firefly version 8.1.0, www http://classic.chem.msu.su/gran/firefly/index.html.

[19] Chemcraft. Version 1.7 (build 132). G.A. Zhurko, D.A. Zhurko. HTML: www.chemcraftprog.com.

[20] Tokarev, K. L. "OpenThermo", v.1.0 Beta 1 (C) ed., 2007-2009. http://openthermo.software.informer.com/.

[21] Gurvich L. V., Yungman V. S., Bergman G. A., Veitz I. V., Gusarov A. V., Iorish V. S., Leonidov V. Y., Medvedev V. A., Belov G. V., Aristova N. M., Gorokhov L. N., Dorofeeva O. V., Ezhov Y. S., Efimov M.E., Krivosheya N. S., Nazarenko I.I, Osina E. L., Ryabova V. G., Tolmach P. I., Chandamirova N. E., Shenyavskaya E.A., "Thermodynamic Properties of individual Substances. Ivtanthermo for Windows Database on Thermodynamic Properties of Individual Substances and Thermodynamic Modeling Software", Version 3.0 (Glushko Thermocenter of RAS, Moscow, 1992-2000).

[22] Ruden, T. A., Taylor, P. R. & Helgaker, T. Automated calculation of fundamental frequencies: Application to AlH_3 using the coupled-cluster singles-and-doubles with perturbative triples method. J. Chem. Phys. 119, 1951 (2003).

[23] Chen, Y. L., Huang, C.-H., Hu, W.-P. & Wei-Ping, H. Theoretical Study on the Small Clusters of LiH, NaH, BeH_2, and MgH_2. J. Phys. Chem. A 109, 9627–9636 (2005).

[24] Wu, C. & Ihle, H. Thermochemistry of the Dimer Lithium Hydride Molecule $Li_2H_2(g)$. ACS Symposium Series, 179, 265–273 (1982).

[25] Graner, G. & Kuchitsu, K. (1998), Structure of Free Polyatomic Molecules: Basic Data, Berlin; New York: Springer.

[26] Tague T. T. Jr & Andrews, L. Reactions of pulsed-laser evaporated boron atoms with hydrogen. Infrared spectra of boron hydride intermediate species in solid argon. J. Am. Chem. Soc. 116(11), 4970–4976 (1994).

[27] Kurth, F. & Eberlein, R. Molecular aluminium trihydride, AlH3: generation in a solid noble gas matrix and characterisation by its infrared spectrum and Ab initio calculations. J. Chem. Soc., Chem. Commun. 16, 1302-1304 (1993).

[28] Jacox, M. "Vibrational and electronic energy levels of polyatomic transient molecules" Monograph 3, J. Phys. Chem. Ref. Data, 461, (1994).

[29] Andrews, L. & Wang, X. Infrared spectra of dialanes in solid hydrogen. J. Phys. Chem. A 108 (19), 4202–4210 (2004).

[30] Gurvich, L. Reference books and data banks on the thermodynamic properties of individual substances. Pure Appl. Chem. 61(6): 027-1031, (1989).

[31] Nakamoto, K. (1986). Infrared and Raman spectra of inorganic and coordination compounds: Wiley Online Library.

[32] Spoliti, M., Sanna, N. & Di Martino, V. Ab initio study on the MBF_4 and $MAlF_4$ molecules. J. Mol. Struct. Theochem 258, 83–107 (1992).

[33] Wang, X., Andrews, L., Tam, S., DeRose, M. E., & Fajardo, M. E. Infrared spectra of aluminum hydrides in solid hydrogen: Al_2H_4 and Al_2H_6. Chem. Soc., 125(30), 9218-9228, (2003).

[34] Linstrom, P. & Mallard, W. NIST chemistry webbook. (2001).